Generalized concept of SH-APM and Love wave sensors

Glen McHale[a)]

School of Science, The Nottingham Trent University, Clifton Lane, Nottingham NG11 8NS, UK

Abstract

An approach to mass and liquid sensitivity for both the phase velocity and insertion loss of shear mode acoustic wave sensors based on the dispersion equations for layered systems is outlined; the approach is sufficiently general to allow for viscoelastic guiding layers. An equation for the phase velocity and insertion loss sensitivities is given which depends on the slope of the complex phase velocity dispersion curves. This equation contains the equivalent of the Sauerbrey and Kanazawa equations for loading of a quartz crystal microbalance by rigid mass and Newtonian liquids, respectively, and also describes surface loading by viscoelastic layers. The theoretical approach can be applied to a four-layer system, with any of the four layers being viscoelastic, so that mass deposition from a liquid can also be modelled. The theoretical dispersion equation based approach to layer-guided shear horizontal acoustic wave modes on finite substrates presented in this work, provides a unified view of Love wave and shear horizontal acoustic plate mode (SH-APM) devices, which have been generally regarded as distinct in sensor research. It is argued that SH-APMs with guiding layers possessing shear acoustic speeds lower than that of the substrate and Love waves are two branches of solution of the same dispersion equation. The layer guided SH-APMs have a phase velocity higher than that of the substrate and the Love waves a phase velocity lower than that of the substrate. Higher order Love wave modes are continuations of the layer guided SH-APMs. The generalized concept of SH-APMs and Love waves provides a basis for understanding the change in sensitivity with higher frequency operation and the relationship between multiple modes in Love wave sensors. It also explains why a relatively thick layer of a high loss polymer can be used as a waveguide layer and so extends the range of materials that can be considered experimentally. Moreover, it is predicted that a new type of sensor, a layer-guided SH-APM sensor, can be constructed in a manner analogous to a Love wave device. The sensitivity of such a device is predicted to approach that of a Love wave sensor whilst retaining the advantage of the SH-APM of using the face opposite the one possessing the transducers as the sensing surface.

Keywords Surface acoustic wave (SAW), Love wave, acoustic plate mode, SH-APM, sensor.
43.35.Pt

[a)] email: glen.mchale@ntu.ac.uk; Tel +44 (0)115 8483383

1 Introduction

Acoustic wave sensors designed for operation in liquid usually use a mode with a shear horizontal polarization in order to avoid the generation of compressional waves in the liquid that would arise from any surface normal displacement [1,2]. The exception to this occurs for flexural plate wave devices, which have a wave speed less than the speed of sound in the liquid and whose vertical component of displacement does not then generate compressional waves [3]. Amongst the most widely used acoustic wave devices is the thickness shear mode (TSM) quartz crystal microbalance (QCM). The shift in resonant frequency, Δf_n, of the quartz crystal to loading by thin layers, Δt_l, of rigidly coupled mass is described by the Sauerbrey equation, $\Delta f_n/f_n=-2f\rho_l\Delta t_l/(\mu_s\rho_s)^{1/2}$ where f is the fundamental resonant frequency, f_n is the resonant frequency of the n^{th} mode (n=1 is the fundamental), μ_s is the shear stiffness of the quartz substrate and ρ_l and ρ_s are the densities of the loading layer and the quartz substrate, respectively [4]. The combination of the loading layer density and the thickness of the layer gives the mass per unit area, $\Delta m_l=\rho_l\Delta t_l$, loading the crystal and hence justifies the term "microbalance". The response of a quartz crystal to immersion in a Newtonian liquid is more complex and involves a frequency shift and a broadening of the resonance, thus indicating both an energy storage and an energy dissipation [5,6]. The prediction of Kanazawa and Gordon was that the frequency shift is given by $\Delta f_n/f_n=-f^{1/2}(\rho_l\eta_l/n\pi\mu_s\rho_s)^{1/2}$, where the ρ_l and η_l are the density and viscosity of the layer. In a liquid the shear mode oscillation of the crystal surface entrains the liquid and the liquid motion has an exponential decay into the liquid of $\exp(-x_3/\delta)$ where x_3 is a coordinate normal to the surface and $\delta=(\eta_l/\pi\ f_n\rho_l)^{1/2}$ is the decay length or shear wave penetration depth. The concept of liquid entrainment enables the Kanazawa and Gordon frequency shift to be written in terms of a frequency dependent interfacial mass loading layer of thickness δ, i.e. $\Delta f_n/f_n=-f\rho_l\delta/(\mu_s\rho_s)^{1/2}$. Modelling of the TSM response to mass loading layers has developed well beyond the simple Sauerbrey and the Kanazawa and Gordon equations and the frequency and damping response of a quartz crystal to single or multiple viscoelastic layers, which contain the rigid mass and Newtonian liquid limits, can now be calculated [7-10]. However, these original equations still provide an important conceptual reference for how solid and liquid properties, and changes in operating frequency, influence acoustic wave response.

The f^2 and $f^{3/2}$ mass and liquid loading frequency responses of the TSM indicates that for higher sensitivity the fundamental frequency should be increased. However, the fundamental frequency corresponds to fitting a half-wavelength standing wave pattern into the crystal thickness. Increasing frequency therefore requires a reduction in crystal thickness and crystals then become fragile. This has motivated the development of surface acoustic wave (SAW) devices which have a wavelength determined by the spacing of the fingers in a surface fabricated interdigital transducer (IDT) [11]. One of the most sensitive of these types of acoustic wave sensors for biosensing uses Love waves [12,13]. Traditionally, a Love wave is a propagating shear mode supported on a semi-infinite substrate possessing a wave-guide overlayer which has an intrinsic shear acoustic speed lower than that of the substrate [14]; in practice a Love wave is created

using a finite thickness substrate (fig. 1a). Other types of acoustic wave sensors utilizing propagating shear modes excited and detected by IDTs include shear horizontal polarized surface acoustic waves (SH-SAWs) and surface transverse waves (STWs). Shear horizontal acoustic plate modes (SH-APMs) are propagating modes involving both the substrate thickness and excitation and detection by IDTs (fig. 1b) [15]. Numerical modelling of mass and liquid response the surface acoustic wave types of sensors is well developed, but tends to be specific to a given device type and does not always provide a simple interpretation.

In this work, we review a dispersion equation based viewpoint of sensor response that provides a common conceptual framework for Love waves and SH-APMs and which is easily extendable to QCM sensors [16-19]. In particular, the dispersion equation approach provides general rules for frequency and mode behavior that should prove useful in designing sensors. The effect of dispersion is possible to understand within this framework and differences between continuous wave and pulse experiments can be predicted [20]. The work also provides a generalisation of the Sauerbrey equation to layer guided shear mode acoustic wave sensors that can be used to evaluate the effect of viscoelasticity in either the layer or the loading medium. One consequence of the dispersion equation approach is the prediction of a new type of layer guided SH-APM sensor, which combines into a single device the higher sensitivity of the Love wave due to layer guiding with the advantage of the SH-APM of being able to use the face opposite the one with the IDTs as the sensor surface.

2 Love Waves on Semi-Infinite Substrates

2.1 The Sauerbrey Equation and Love Wave Mass Sensitivity

The TSM based quartz crystal microbalance provides a simple model for understanding mass sensitivity. Consider a quartz crystal of thickness t_s operating at its fundamental frequency, f_o, so that the upper and lower surfaces are antinodes in the displacement and the crystal thickness is related to the wavelength by $\lambda_o=2t_s$. The wave must satisfy the equation $v_s=f_o\lambda_o$ where $v_s=(\mu_s/\rho_s)^{1/2}$ is the intrinsic speed of shear waves in the substrate. To obtain the frequency based mass sensitivity, imagine depositing a thin layer, Δt_s, of quartz on the quartz substrate. The equation $v_s=f\lambda$ must still be satisfied, but with changes in the wavelength compensated by changes in the frequency, i.e. $v_s=(f_o+\Delta f)(\lambda_o+\Delta\lambda)$, so that to first order,

$$\frac{\Delta f}{f_o} \approx -\frac{\Delta\lambda}{\lambda_o} \tag{1}$$

However, we also know that, prior to deposition of the thin layer, the substrate thickness was half a wavelength and that the wavelength was given by the shear speed divided by the frequency, so that we can write,

$$\frac{\Delta f}{f_o} \approx -\frac{2\rho_s \Delta t_s f_o}{\sqrt{\mu_s \rho_s}} \tag{2}$$

Defining the frequency based mass sensitivity as,

$$S_m^f \equiv \lim_{\Delta m \to 0} \frac{1}{\Delta m}\left(\frac{\Delta f}{f_o}\right) \tag{3}$$

and recognizing that in Eq. (2), $\Delta m = \rho_s \Delta t_s$ we obtain the sensitivity of the TSM,

$$S_m^f \approx -\frac{2 f_o}{\sqrt{\mu_s \rho_s}} \tag{4}$$

Eq. (4) can be regarded as the sensitivity of the crystal towards a layer of any material provided that material is thin enough. Significantly, Eq. (4) depends only upon the properties of the substrate and the operating frequency, f_o.

The relevance to layer-guided acoustic waves, such as Love waves, of the argument used in deriving Eq. (4) is in how we interpret the dispersion curve. If we can solve the wave equations for a layered system with specific boundary conditions, then mass and liquid sensitivity of the phase velocity, which can be complex if damping is present in any layer, will depend upon the changes that occur by increasing a layer by an infinitesimal amount [18,19]. The sensitivity function will not depend on the perturbing layer properties, but only on the properties of the original substrate and guiding layer, and the operating frequency; this should be valid at least to a first approximation. Another way of stating the above is to note that if we can obtain theoretically from the dispersion equation, the graph of the phase speed dependence on layer thickness then we can predict the mass sensitivity of a device. Alternatively, if the phase speed dependence on layer thickness is known experimentally then we can predict the mass sensitivity of a device. Consider the Love wave dispersion curves shown in fig. 2 for the first three Love wave modes on an infinitely thick substrate possessing a shear speed of v_s=5100 ms^{-1} and coated with a guiding layer possessing a shear speed of v_l=1100 ms^{-1}. For illustrative purposes this calculation corresponds to propagation orthogonal to the crystalline X direction on a polymer coated ST-cut quartz substrate. The horizontal axis in fig. 2 uses a normalized scale of $z=d/\lambda_l$ where $\lambda_l = v_l/f$ and is therefore frequency dependent. For any given substrate, the operating frequency, f_o, and guiding layer thickness, d, determine an operating point, z_o, on the dispersion curve. If, having chosen the operating point, we now imagine depositing a thin layer, Δt_l, of the same material as the guiding layer onto the guiding layer, the operating point z_o will move along the horizontal axis. The net effect will be to reduce the phase speed by an amount Δv from the phase speed, v_o, at the original operating point. The larger the slope of the dispersion curve at the original operating point, the larger the fractional change in phase speed and the larger the phase velocity defined mass sensitivity. This idea has been developed rigorously and the result for the mass sensitivity of a Love wave device can be expressed by the equation [18,19],

$$S_m^v \equiv \lim_{\Delta m \to 0} \frac{1}{\Delta m}\left(\frac{\Delta v}{v_o}\right) \approx \left[\frac{1 - v_p^2/v_o^2}{1 - v_l^2/v_o^2}\right] \frac{f_o}{\sqrt{\mu_l \rho_l}} \left(\frac{d \log_e v}{dz}\right)_{z_o} \qquad (5)$$

where $v_p=(\mu_p/\rho_p)^{1/2}$ is the intrinsic speed of shear waves in the perturbing material; when the perturbing material is the same material as the layer the factor in square brackets is unity. Eq. (5) is an analogue to the Sauerbrey result (Eq. (4)) and indicates that the fractional shift in phase speed of a Love wave device is proportional to the operating frequency, f_o, and the local slope of the dispersion curve at the operating point, z_o. This local slope may itself be frequency dependent and so it would not be correct to conclude that, in general, the sensitivity is necessarily proportional to the operating frequency.

Figure 3 shows the mass sensitivity curves from Eq. (5) corresponding to the data in fig. 2. For each mode there is a maximum phase speed sensitivity corresponding to the operating point z being at the point of maximum slope in the dispersion curves. A physical interpretation of the mass sensitivity arising from the Love wave dispersion curve is that the point of steepest slope corresponds to the device being placed at the transition point for the wave displacement being dominantly in the substrate to dominantly in the guiding layer. When the Love wave displacement is dominantly in the substrate its phase speed is close to that of a shear wave in the substrate (i.e. $v \sim v_s$). In contrast, when the Love wave displacement is dominantly in the guiding layer its phase speed is close to that of a shear wave in the guiding layer (i.e. $v \sim v_l$). The high mass sensitivity of the Love wave does not therefore arise because the wave has been fully localized in the guiding layer, but because the wave is on the transition point whereby mass added to the guiding layer will rapidly cause the wave to become fully localized to the guiding layer [18,19].

2.2 Polymer Guiding Layer

The interpretation developed for phase speed mass sensitivity in a Love wave device also suggests that by using a polymer guiding layer the insertion loss can, in principle, be a good sensor parameter [19]. How effectively the principle could be applied depends on the relative precision that could be obtained practically compared to a frequency or phase measurement. When the Love wave displacement is dominantly in the substrate the loss is relatively low, but when mass is added to the guiding layer surface the operating point moves down the complex phase velocity dispersion curve and the Love wave displacement becomes dominantly in the layer. If this guiding layer is a polymer, a large change in insertion loss will arise even if the sensed material itself is rigid mass. In a Maxwell model for the viscoelasticity of the guiding layer the insertion loss per metre propagation path, IL, on localization in the guiding layer becomes,

$$IL = -20(\log_{10} e)\,\mathrm{Im}\left[\frac{\omega}{v}\right] \to 20(\log_{10} e)\left(\frac{\omega}{v_l^\infty}\right)\sqrt{\frac{1+(\omega\tau)^2}{2\omega\tau}}\,F_{-}(\omega\tau) \qquad (6)$$

where $\omega=2\pi f$ is the angular frequency, $\tau=\eta_l/\mu_l$ is the Maxwellian relaxation time and the superscript in v_l^{∞} implies the solid limit for a viscoelastic guiding layer (i.e. $v_l^{\infty}=[G_l(\omega\tau\to\infty)/\rho_l]^{1/2}$ where G_l is the shear modulus of the guiding layer). The function $F_{\pm}(\omega\tau)$ is given by,

$$F_{\pm}(\omega\tau)=\left(\frac{\sqrt{1+(\omega\tau)^2}\pm\omega\tau}{1+(\omega\tau)^2}\right)^{1/2} \tag{7}$$

so that for thick guiding layers (i.e. d such that $v\to v_l$) and $\omega\tau>>1$, $IL\propto(\omega\tau)^{-1}$. Figure 4 shows the insertion loss as a function of normalized guiding layer thickness $z^{\infty}=d/\lambda_l^{\infty}$ where $\lambda_l^{\infty}=v_l^{\infty}/f$ calculated using $\omega\tau=10^4$ and a frequency of 100 MHz. The horizontal dotted line is the result from Eq. (6). The implication from fig. 4 is that an insertion loss mass sensitivity can be defined in a similar manner to a phase velocity mass sensitivity and that changes in insertion loss can be used to monitor both deposition of rigid mass from the vapor or liquid phase and changes in liquid viscosity-density.

2.3 Frequency Hopping

Considering the dispersion equation graph for the case of a mass based guiding layer on a semi-infinite substrate, it is possible to understand the effect of higher frequency or thicker guiding layers on the mass sensitivity of a Love wave device [18]. Two possible routes to higher frequency operation are: i) to increase the fundamental frequency, and ii) to use IDTs capable of working at harmonic frequencies. In both cases, Eq. (5) shows that if the guiding layer thickness is reduced inversely proportional to the frequency, so that the operating point z_o does not alter, then the phase velocity mass sensitivity will scale directly with frequency. However, if the operating frequency is increased whilst retaining the guiding thickness at a constant value, e.g. by using a harmonic of the IDT operating frequency, then several possibilities can occur. An increase in frequency may result in a new operating point on the dispersion curve with an increased or decreased slope and may also result in a change in the Love wave mode; several of these possibilities are shown in fig. 5. In each of the example cases a)-d) the normalized guiding layer thickness z_o, defining the operating point, is increased by increasing the operating frequency. Transition a) will result in an increased phase velocity mass sensitivity because both the slope factor and the explicit frequency factor in Eq. (5) increase. However, transitions b)-d) all result in lower slopes at the new operating points on the dispersion curves and, of these, only transition d) has a sufficient increase in operating frequency to overcome the reduction in slope. Thus, increasing the operating frequency for a Love wave device may or may not result in higher mass sensitivity. The issue of change of Love wave mode is particularly important for a polymer based guiding layer as in this case transition c), rather than transition b), would be expected due to the high insertion loss for a fully localized Love wave mode.

3 Layer-guided Waves on Finite Thickness Substrates

3.1 Generalized Sauerbrey Equation

The result in Eq. (5) can be extended to the loading by a finite thickness viscoelastic fluid of density ρ_f, thickness h and complex shear speed $v_f=(G_f/\rho_f)^{1/2}$, where G_f is the complex shear

modulus, of a polymer waveguide layer on a finite thickness substrate [19]. The fractional change in phase speed is then,

$$\frac{\Delta v}{v_o} \approx \left(\frac{1 - v_f^2 / v_o^2}{1 - v_l^2 / v_o^2} \right) \left(\frac{d \log_e v}{dz} \right)_{z=z_o} \left(\frac{\tan\left(T_f^o h\right)}{T_f^o h} \right) \frac{\rho_f h f_o}{\sqrt{G_l(\omega\tau \to \infty)\rho_l}} \tag{8}$$

where the wavevector T_f^o is given by,

$$T_f^0 = \omega_o \left(\frac{1}{v_f^2} - \frac{1}{v_o^2} \right)^{1/2} \tag{9}$$

It should be noted that both the slope term in Eq. (8) and the operating point phase speed v_o in Eq. (9) depend on the operating frequency f_o. The similarity of Eq. (8) to the Sauerbrey, and Kanazawa and Gordon equations can be seen by noting that in the Maxwell model for a viscoelastic loading the tan$x$/x type factor in Eq. (8) has the solid and liquid limits given by,

$$\left(\frac{\tan\left(T_f^o h\right)}{T_f^o h} \right) \to \begin{cases} 1 & h \to 0 \\ \dfrac{\sqrt{-2j}}{2h\left(1 - v_f^2 / v_o^2\right)^{1/2}} \sqrt{\dfrac{2\eta_f}{\omega_o \rho_f}} & h \to \infty \quad \text{and} \quad \omega_o \tau \to 0 \end{cases} \tag{10}$$

where ω_o is the angular frequency and $\tau = \eta_f / \mu_f$ is the Maxwellian relaxation time for the loading layer. In the thin solid limit tan$x$/$x \to 1$ and $\Delta v / v_o \propto \rho_f h$ so that the fractional shift in phase speed is proportional to the deposited mass per unit area. In this limit, providing the guiding layer is composed of rigid mass, only a real velocity shift arises. The explicit frequency dependence of the $\Delta v / v_o$ is also proportional to frequency, although the slope factor will introduce an additional frequency dependence. In the limit of an infinitely deep Newtonian liquid Eq. (8) has a dependence on the square root of the density-viscosity product, i.e. $(\rho_f \eta_f)^{1/2}$, and the explicit frequency dependence is reduced to $f_o^{1/2}$, although again the slope factor will introduce an additional frequency dependence. In addition the $(-2j)^{1/2}$ means that the $\Delta v / v_o$ response to a Newtonian liquid includes a damping term even if the guiding layer is composed of rigid mass. The change in insertion loss per unit propagation length due to a small change in the (complex) phase velocity can be calculated from Eq. (8) using,

$$\Delta IL = 20\left(\log_{10} e\right) \mathrm{Im}\left[\frac{\omega_o}{v_o} \left(\frac{\Delta v}{v_o} \right) \right] \tag{11}$$

3.2 Layer-Guided SH-APMs

Up to this stage in this work, the dispersion equation has been used primarily as a tool to understand traditional Love wave devices composed of a guiding layer on a semi-infinite

substrate. However, in any experiment a finite thickness substrate is used and the results in section 3.1 are sufficiently general to be accurate in this case. Consider again fig. 1a) for a Love wave device using a finite substrate and fig. 1b) for a SH-APM device. These sensor devices have many common features: both use IDTS to excite propagating waves with shear displacements parallel to the surface and, when the SH-APM is used as a sensor, both will have a layer on one surface. The difference between the devices is that the Love wave displacement has an antinode at the top surface of the layer and decays with depth into the substrate whereas the SH-APM has antinodes at both the top surface of the layer and at the lower surface of the substrate. Thus, within a model neglecting electric field effects, it is possible to use a common set of equations of motion and boundary conditions to describe both the Love wave on a finite substrate and the SH-APM with a guiding layer [16,17]. In this approach, the substrate and layer solutions can be written in the forms,

$$\underline{u}_s = (0,1,0)\left[C_s e^{-T_s x_3} + D_s e^{T_s x_3}\right] e^{j(\omega t - k_1 x_1)} \tag{12}$$

$$\underline{u}_l = (0,1,0)\left[A_l e^{-jT_l x_3} + B_l e^{jT_l x_3}\right] e^{j(\omega t - k_1 x_1)} \tag{13}$$

where the subscripts s and l indicate substrate and guiding layer, and $k_1=(\omega/v)$ gives the phase speed, v, of the solution. Substituting these solutions into the equations of motion for the substrate and guiding layer materials and applying boundary conditions gives a dispersion equation for the system of shear mode propagation on the substrate with the guiding layer. This approach has been developed to describe a system a substrate plus three viscoelastic layers [19]. Since in the extreme relaxation time limits a viscoelastic layer can be regarded either as rigid mass or as a Newtonian liquid, the developed model has wide applicability. For example, with four layers, the first two layers could represent the substrate and guiding layers, the fourth layer could represent a liquid in which a device was immersed and the third layer could represent mass deposited from the liquid phase. Increasing the model to more than four layers is straightforward in principle, but involves additional algebraic complexity.

In the simplest case of a substrate of thickness, w, overlayed with a single layer of rigid mass of thickness, d, applying the boundary conditions gives a dispersion equation,

$$\tan(T_l d) = \xi \tanh(T_s w) \tag{14}$$

where ξ is defined as,

$$\xi = \frac{\mu_s T_s}{\mu_l T_l} \tag{15}$$

Figure 6 shows the numerical calculation of the full spectrum for the solution of the dispersion equation, Eq. (14), for a frequency of 100 MHz. In contrast to the calculation in fig. 3, the curves in fig. 6 are only valid for the specific frequency of the calculation. The thickness of the

substrate, w, determines the number of Love wave modes and the spacing of the associated acoustic plate modes. At the start of each successive Love wave mode the phase speed of the Love wave is $v=v_s$ and the speeds of the associated plate modes are $v_m=v_s/(1-(m\pi v_s/w\omega)^2)^{1/2}$, where m=1, 2, 3, … . Significantly, from Eq. (14), the wavevector T_s can be real or imaginary with the real solution corresponding to $v<v_s$ and the imaginary solution corresponding to $v>v_s$. Plots of the displacements show that the real solutions for T_s have displacements decaying into the substrate (i.e. Love wave type behavior) whereas the imaginary solutions for T_s have displacements representing substrate resonances (i.e. SH-APMs) [17]. Because both types of solution fully satisfy the boundary conditions at both the upper and lower faces, it means that there is no requirement for a critical penetration depth on the finite substrate for the Love wave type solution to exist. Thus, in fig. 6 the curves beginning with phase speeds higher than 5100 ms^{-1} correspond to SH-APM type solutions with guiding layers and those with phase speeds lower than 5100 ms^{-1} correspond to Love wave type solutions on finite thickness substrates.

The guiding layer thickness can be chosen to simultaneously satisfy both the Love wave condition $\tan(T_l d)=0$ and the SH-APM condition $\tan(k_s w)=0$, where $T_s=jk_s$, by choosing a thickness d_{nm} given by,

$$\frac{d_{nm}}{\lambda_l}=\frac{n}{2\sqrt{1-\left(\frac{v_l}{v_s}\right)^2\left[1-\left(\frac{m\lambda_s}{2w}\right)^2\right]}} \tag{16}$$

where n=0,1,2,3, …. labels the successive Love wave modes and $\lambda_s=v_s/f$. The start of each Love wave mode and the start of each associated plate mode are shown by the solid circles in fig. 6. As the guiding layer thickness increases, the n=0 Love wave evolves into a displacement with a single node located close to the substrate-layer interface and an antinode at the surface of the guiding layer. Each higher order Love wave introduces an additional node within the layered system. Graphical illustrations showing how the displacements evolve as the guiding layer thickness increases are given in reference [17]. This theoretical approach therefore provides a combined model of Love wave and SH-APM sensors and predicts that layer-guiding is possible for SH-APMs and that layer guided SH-APMs evolve into Love wave modes as the guiding layer thickness is increased. Previously published work has also shown that the approach can incorporate SH-SAWs [19]. It has also provided a range of analytical approximations for sensitivity of all these devices with viscoelastic guiding layers to deposition of rigid and non-rigid mass from the vapor/liquid phase and to liquid properties.

In the previous sections, it was shown that the dispersion equation provided a powerful tool for understanding the sensitivity of Love wave devices. It can be shown that Eq. (8) continues to be valid for both the layer-guided SH-APMs and the Love waves on a finite substrate. Thus, the slope at the operating point of the dispersion curve determines the sensitivity of a device. An immediate consequence is that by introducing a guiding layer, a significant enhancement in the

mass/liquid sensitivity can be achieved for a SH-APM device. Indeed, the effect on a given mode of a SH-APM device of increasing the guiding layer thickness is to eventually cause a step-like transition in the phase speed down to that of the next mode. The separation in phase speeds of the two highest SH-APM modes can be larger than the difference between the substrate and guiding layer speeds between which the Love wave makes a step-like transition. Thus, a layer-guided SH-APM device with a sensitivity approaching that of a Love wave device may be possible. Fig. 7 shows the SH-APM mass sensitivities corresponding to fig. 6; the zero thickness guiding layer limit mass sensitivities for the three $n>0$ SH-APM modes are 3.85, 4.92 and 8.91 m^2 kg^{-1}, respectively. The peak increase in mass sensitivity of the SH-APMs due to an optimum guiding layer thickness is several orders of magnitude for the highest mode, but not quite as high as the mass sensitivity of the Love wave modes (see fig. 3)

4 Conclusions and Experimental Implications

The purpose of this work has been to provide a conceptual framework in which the behavior of a wide range of acoustic wave sensors employing guiding layers can be understood. Although the focus of this work has been on Love wave and layer-guided SH-APM devices, the methodology used can be applied to the frequency response of TSM quartz crystal resonators. Experimentally, for Love wave devices using polymers the existence of multiple Love wave modes has been confirmed, as has the change in phase speed mass sensitivity [21,22]. Higher order Love wave modes have potential for sensors using alternative guiding layer materials which may need to be thicker, an example would be a molecularly imprinted polymer used as both a selective and a guiding layer [23]. The relationship between sensitivity and frequency is potentially useful because it provides predictions of how to design devices with optimum sensitivity. Examples include scaling guiding layer thickness inversely with frequency and using third, but not second, harmonic frequency transducers to hop between the optimum sensitivity of the first and third modes; it should be noted that the frequency change needs to be slightly greater than a factor of three [18]. Hopping between frequencies may provide a route to examining relaxation time effects in polymers films or liquids [24,25]. For viscoelastic guiding layers, it is possible to understand why an insertion loss response may arise even when the deposition sensed is of rigid mass. Thus, the theory suggests that an experimental focus solely on phase velocity changes is too restrictive. The change in insertion loss with guiding layer thickness predicted by the theory is qualitatively correct for Love wave devices created by using a substrate supporting a pure SH-SAW, such as 36^o YX-$LiTaO_3$ with a metallized path. However, it does not correctly predict the initial insertion loss behavior with guiding layer thickness for devices constructed on a substrate using a surface skimming bulk wave (SSBW), such as propagation orthogonal to the X-axis on ST-cut quartz [22]. Experimentally, the initial effect of a guiding layer on such a substrate is to effectively short circuit some of the SSBW attenuation. Nonetheless, the idea of sensitivity being related to the slope of the experimentally determined dispersion curve remains relevant to the initial behavior of the insertion loss for such devices and the concepts developed in this work explain the multiple mode behavior of such devices. Whilst not discussed in this work, the dispersion curve is also useful in relating group velocity to the mass sensitivity and understanding pulse mode based sensors [21,26]. One of the strongest predictions of the dispersion curve

approach to Love wave sensors has been to unite their treatment with that of SH-APM sensors. This has resulted in the prediction that a guiding layer can significantly enhance sensitivity of SH-APM devices; similar effects can be anticipated for TSM quartz crystal resonators. The experimental confirmation of the prediction of sensitivity enhancement due to the guiding layer has been obtained and it has been shown to remain effective for the SH-APM even when the face used for sensing is on the opposite side to that containing the IDTs [22,27]. Thus, it should be possible to construct devices having a sensitivity approaching that of Love wave devices, but without the problems of liquids and liquid seals on the same face as the transducers.

Acknowledgements
The author gratefully acknowledges the BBSRC for financial support under research grant 301/E11140. Dr M. I. Newton and Dr F. Martin are acknowledged for their invaluable supporting experimental work and discussions, which have helped to develop the ideas of guided plate modes.

References

[1] D. S. Ballantine, R. M. White, S. J. Martin, A. J. Ricco, E. T. Zellers, G. C. Frye, and H. Wohjlten, "*Acoustic wave sensors*" (Academic, New York, 1997)

[2] M. Thompson and D. C. Stone, "*Surface-launched acoustic wave sensors*" (John Wiley and Sons, New York, (1997).

[3] R. M. White, Faraday Discuss. 107, 1 (1997).

[4] G. Z. Sauerbrey, Z. Phys. 155, 206 (1959).

[5] K. K. Kanazawa and J. G. Gordon, II, Analytica Chimica Acta 175, 99 (1985).

[6] S. Bruckenstein and M. Shay, Electroch. Acta. 30, 1295 (1985).

[7] A. R. Hillman, A. Jackson and S. J. Martin, Anal. Chem. 73, 540 (2001).

[8] S. J. Martin, H. L. Bandey, R. W. Cernosek, A. R. Hillman and M. J. Brown, Anal. Chem. 72, 141 (2000).

[9] H. L. Bandey, S. J. Martin, R. W. Cernosek and A. R. Hillman, Anal. Chem. 71, 2205 (1999).

[10] C. Behling, R. Lucklum and P. Hauptmann, IEEE Trans. Ferroel. Freq. Ctrl. 46, 1431 (1999).

[11] M. J. Vellekoop, Ultrasonics, 36, 7 (1998).

[12] E. Gizeli, A. C. Stevenson, N. J. Goddard, and C. R. Lowe, IEEE Trans. Ultrason. Ferroelectr. Freq. Control 39, 657 (1992).

[13] G. Kovacs and A. Venema, Appl. Phys. Lett. 61, 639 (1992).

[14] D. P. Morgan, "*Surface-wave Devices for Signal Processing*", (Elsevier, New York, 1991)

[15] S. J. Martin, A. J. Ricco, T. M. Niemczyk and G. C. Frye, Sens. Act. 20, 253 (1989).

[16] M. I. Newton, G. McHale, F. Martin, E. Gizeli, and K. A. Melzak, Europhys. Lett. 58, 818 (2002).

[17] G. McHale, M. I. Newton, and F. Martin, J. Appl. Phys. 91, 5735 (2002).

[18] G. McHale, M. I. Newton, and F. Martin, J. Appl. Phys. 91, 9701 (2002).

[19] G. McHale, M. I. Newton, and F. Martin, J. Appl. Phys. 93 , 675 (2003).

[20] G. McHale, F. Martin and M.I. Newton, J. Appl. Phys. 92, 3368 (2002).

[21] G. McHale, M. I. Newton, F. Martin, K. A. Melzak, and E. Gizeli, Appl. Phys. Lett. 79, 3542 (2001).

[22] F. Martin, "*Layer-guided shear acoustic wave sensors*", Ph.D Thesis, The Nottingham Trent University (2002).

[23] B. Jakoby, G. M. Ismail, M. P. Byfield and M. J. Vellekoop, Sens. Act. A 76, 93 (1999)

[24] M. I. Newton, F. Martin, K. A. Melzak, E. Gizeli and G. McHale, Electron. Lett. 37, 340 (2001).

[25] M. Weiss, W. Welsch, M. v. Schickfus and S. Hunklinger, Anal. Chem. 70, 2881 (1998).

[26] M.I. Newton, G. McHale, F. Martin, E. Gizeli and K.A. Melzak, Analyst 126, 2107 (2001).

[27] M.I. Newton, F. Martin and G. McHale, Appl. Phys. Lett. 82 2181 (2003).

Figure Captions

Figure 1
a) Love wave device, b) SH-APM device. In both cases the displacements for the first mode are shown schematically.

Figure 2
Phase speed variation with normalized guiding layer thickness $z=d/\lambda_l$, where $\lambda_l = v_l/f$, for the first three Love wave modes; the solid circles are analytical results. The parameters used in the calculation are v_s=5100 m s^{-1}, v_l=1100 m s^{-1}, ρ_s=2655 kg m^{-3} and ρ_l=1000 kg m^{-3}, and the guiding layer is assumed to be rigid mass and the substrate of semi-infinite thickness.

Figure 3
Mass sensitivity (Eq. (5)) as a function of normalized guiding layer thickness $z=d/\lambda_l$, for the Love wave modes shown in fig. 2.

Figure 4
The insertion loss as a function of normalized guiding layer thickness $z^{\infty}=d/\lambda_l^{\infty}$ where $\lambda_l^{\infty} = v_l^{\infty}/f$ using a viscoelastic guiding layer with $\omega\tau=10^4$ and a frequency of 100 MHz; other parameters are the same as in fig. 2. The horizontal dotted line is the limiting result from Eq. (6).

Figure 5
Illustrations of possible changes in Love wave operating point and mode due to a frequency increase. Transitions a) and d) both give increased mass sensitivity whereas transitions b) and c) result in lower mass sensitivity.

Figure 6
Phase speed variation with normalized guiding layer thickness $z=d/\lambda_l$, where $\lambda_l = v_l/f$, for the first three Love wave modes and associated SH-APMs on a finite thickness substrate; the solid circles are analytical results. The parameters used in the calculation are v_s=5100 ms^{-1}, v_l=1100 ms^{-1}, ρ_s=2655 kg m^{-3}, ρ_l=1000 kg m^{-3} and w=100 μm, and the guiding layer is assumed to be rigid mass.

Figure 7
Mass sensitivity (Eq. (5)) as a function of normalized guiding layer thickness $z=d/\lambda_l$, for the SH-APMs shown in fig. 6. The mass sensitivity of the corresponding Love wave modes is similar to that shown in fig. 3.

McHale - Generalized concept of SH-APM and Love wave sensors

Figure 1

a) Love wave device, b) SH-APM device. In both cases the displacements for the first mode are shown schematically.

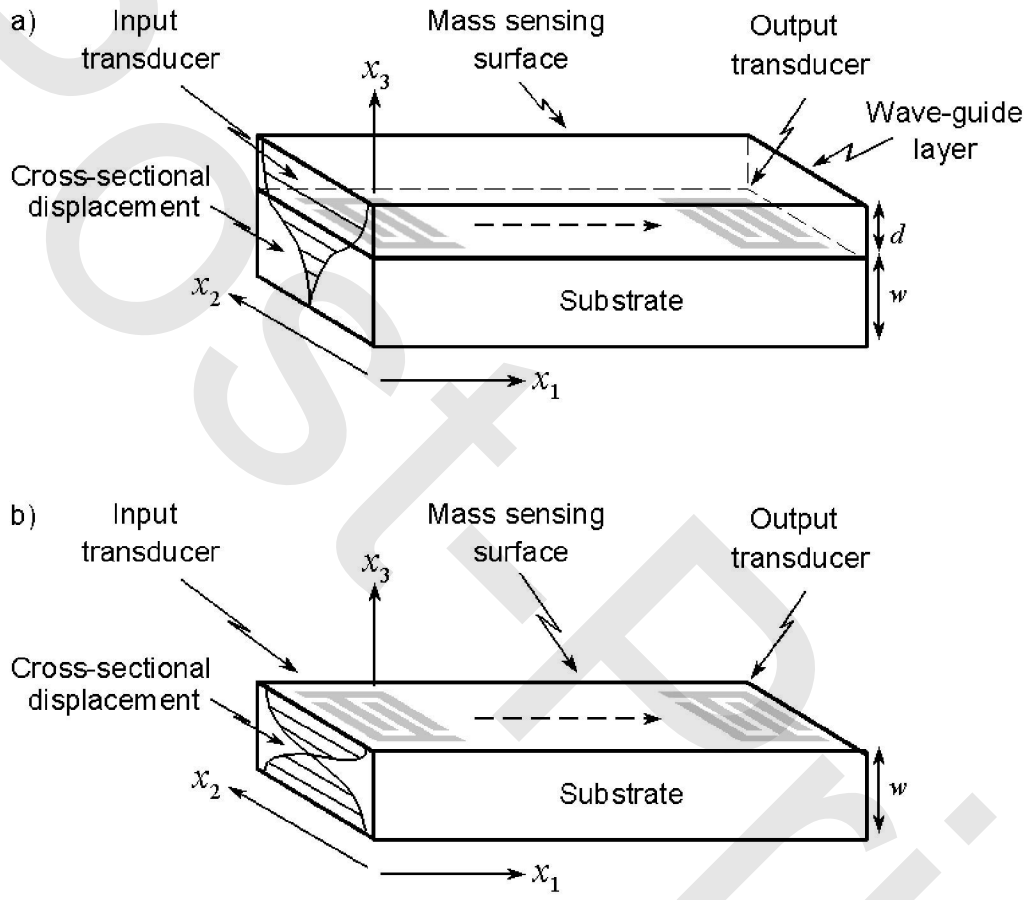

Figure 2

Phase speed variation with normalized guiding layer thickness $z=d/\lambda_l$, where $\lambda_l = v_l/f$, for the first three Love wave modes; the solid circles are analytical results. The parameters used in the calculation are v_s=5100 m s^{-1}, v_l=1100 m s^{-1}, ρ_s=2655 kg m^{-3} and ρ_l=1000 kg m^{-3}, and the guiding layer is assumed to be rigid mass and the substrate of semi-infinite thickness.

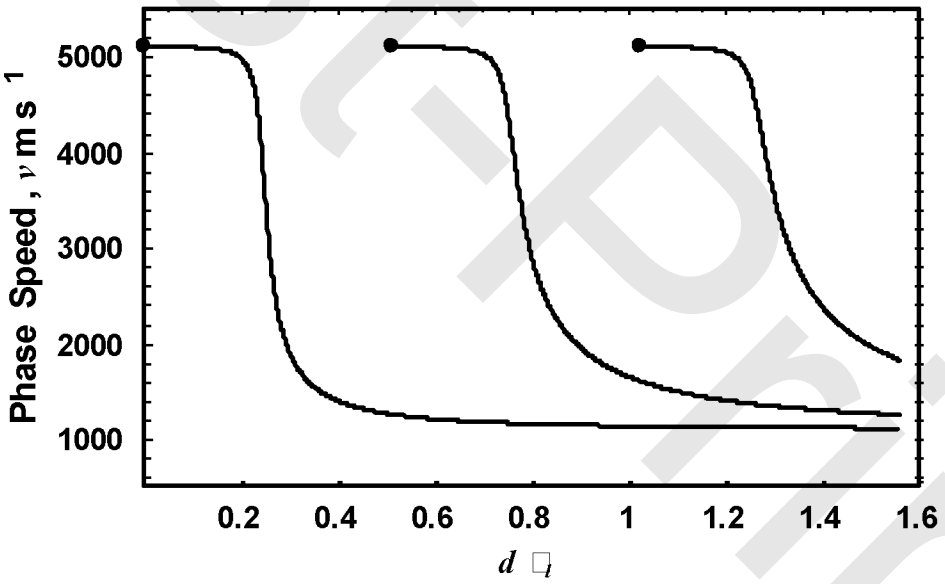

Figure 3
Mass sensitivity (Eq. (5)) as a function of normalized guiding layer thickness $z=d/\lambda_l$, for the Love wave modes shown in fig. 2.

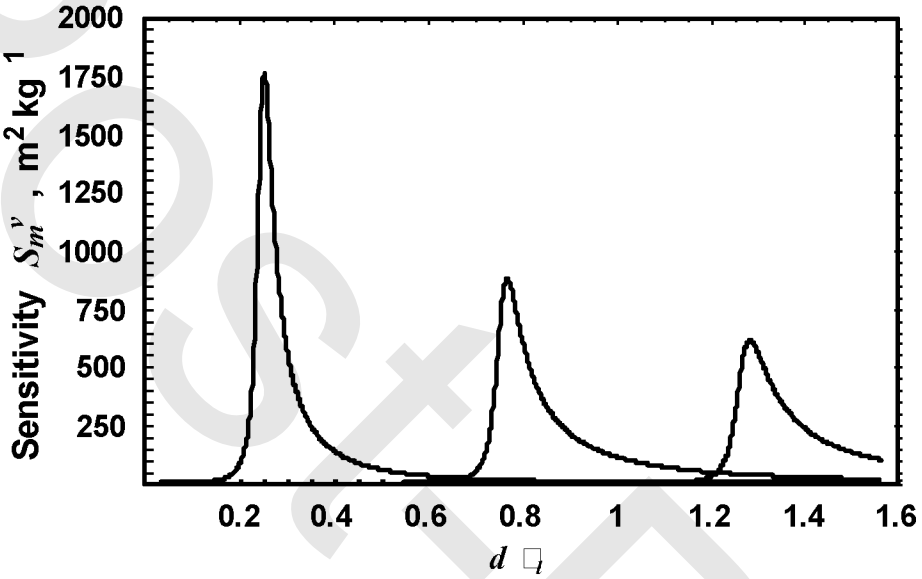

Figure 4

The insertion loss as a function of normalized guiding layer thickness $z^{\infty}=d/\lambda_l^{\infty}$ where $\lambda_l^{\infty}= v_l^{\infty}/f$ using a viscoelastic guiding layer with $\omega\tau=10^4$ and a frequency of 100 MHz; other parameters are the same as in fig. 2. The horizontal dotted line is the limiting result from Eq. (6).

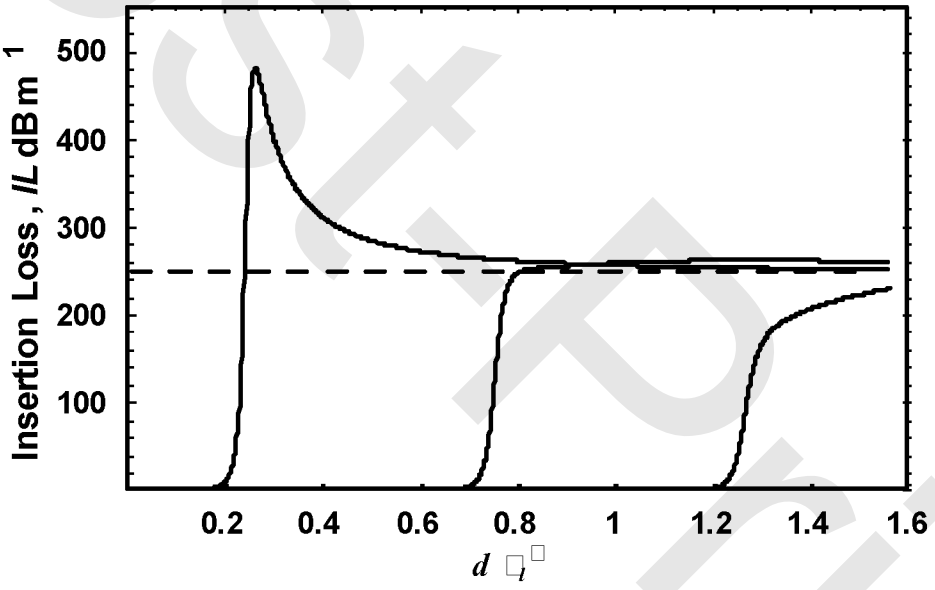

Figure 5
Illustrations of possible changes in Love wave operating point and mode due to a frequency increase. Transitions a) and d) both give increased mass sensitivity whereas transitions b) and c) result in lower mass sensitivity.

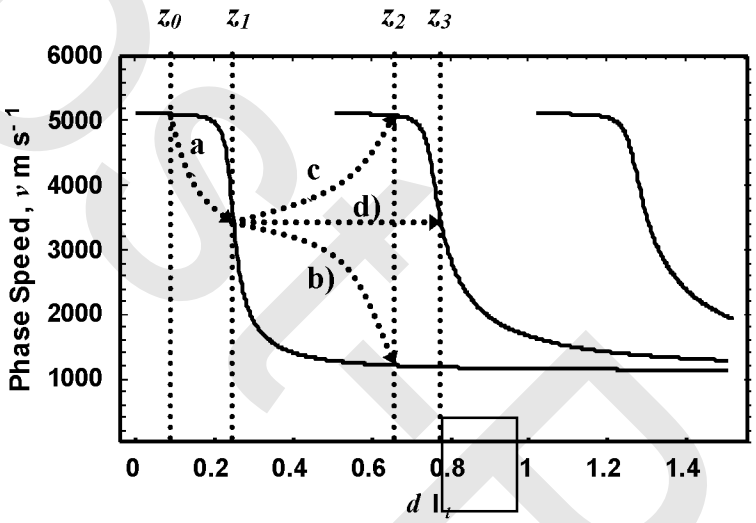

Figure 6

Phase speed variation with normalized guiding layer thickness $z=d/\lambda_l$, where $\lambda_l = v_l/f$, for the first three Love wave modes and associated SH-APMs on a finite thickness substrate; the solid circles are analytical results. The parameters used in the calculation are v_s=5100 ms^{-1}, v_l=1100 ms^{-1}, ρ_s=2655 kg m^{-3}, ρ_l=1000 kg m^{-3} and w=100 μm, and the guiding layer is assumed to be rigid mass.

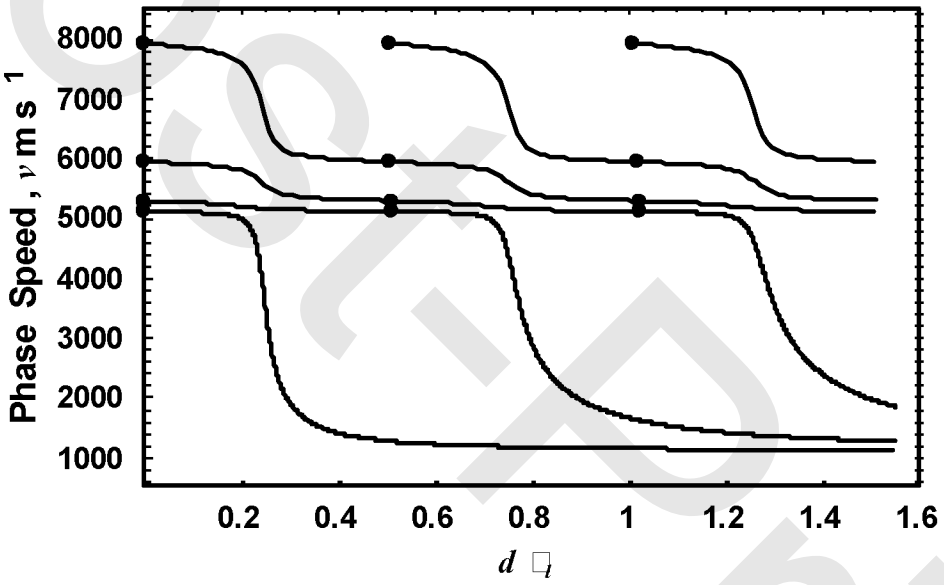

Figure 7
Mass sensitivity (Eq. (5)) as a function of normalized guiding layer thickness $z=d/\lambda_l$, for the SH-APMs shown in fig. 6. The mass sensitivity of the corresponding Love wave modes is similar to that shown in fig. 3.